04 Apr 1995, 10:30 am - 12:00 pm

Three-Dimensional Cyclic Behaviour of Interfaces

E. Evgin
University of Ottawa, Canada

K. Fakharian
University of Ottawa, Canada

Proceedings: Third International Conference on Recent Advances in Geotechnical Earthquake Engineering and Soil Dynamics,
April 2–7, 1995, Volume I, St. Louis, Missouri

Three-Dimensional Cyclic Behaviour of Interfaces

Paper No. 1.04

E. Evgin
Associate Professor of Civil Engineering, University of Ottawa, Ottawa, Ontario, Canada

K. Fakharian
Graduate Student of Civil Engineering, University of Ottawa, Ottawa, Ontario, Canada

SYNOPSIS A new apparatus is used to study the behaviour of an interface between dry sand and a rough surface under three-dimensional cyclic loading conditions. A simple shear type of soil container is utilized in the experiments to investigate the coupling effects of two orthogonal shear stresses acting on the interface. The significance of the results are discussed with reference to the behaviour of axially-laterally loaded piles.

INTRODUCTION

Various types of devices are described in the literature for testing interfaces between soil and structural materials including the direct shear type (Desai 1981, Boulon and Plytas 1986), ring torsion type (Yoshimi and Kishida 1981), and simple shear type (Uesugi and Kishida 1986). The tests conducted by using all these devices are only two dimensional (2-D), where a normal force and a tangential force are applied to the interface plane.

A direct shear type apparatus for three-dimensional (3-D) testing of interfaces is described by Fakharian and Evgin (1993). This apparatus (Fig. 1) is capable of applying monotonic and cyclic loads in three orthogonal directions, i.e. a force normal to the interface plane, and two tangential forces in the plane of the interface. The operation of the apparatus and data acquisition are fully computer controlled. The same apparatus is modified by manufacturing a simple shear type of soil container and it is used to study the behaviour of an interface under 3-D cyclic loading conditions.

In many soil-structure systems, the interface is subjected to 3-D stress conditions as shown in Fig. 2. In a special case of loading, interface may be subjected to a normal stress, σ_n, and a constant shear stress, τ_y, while it is sheared in the x-direction under cyclic loading conditions. A pile carrying both axial and lateral loads is a typical example of such a case. Smith and Ray (1986) pointed out that a laterally loaded pile derives most of its resistance from frontal resistance and from frictional resistance. At working loads, the side friction provides the majority of the resistance. Figure 3 shows a typical infinitesimal interface element, e, on a pile shaft which is subjected to a normal stress, σ_n, resulting from the lateral pressure of the surrounding soil, a shear stress in the axial direction, τ_{axi}, resulting from both axial and lateral loads, and a second shear stress induced by the lateral load, τ_{lat}. In reference to the interface experiments presented here, τ_{axi} and τ_{lat} are referred to as τ_y and τ_x, respectively.

This paper describes a series of cyclic 3-D tests between a dry sand and a rough surface. These tests are part of an experimental work to investigate the coupling effects between the two orthogonal shear stresses in the x and y directions (Fakharian 1994).

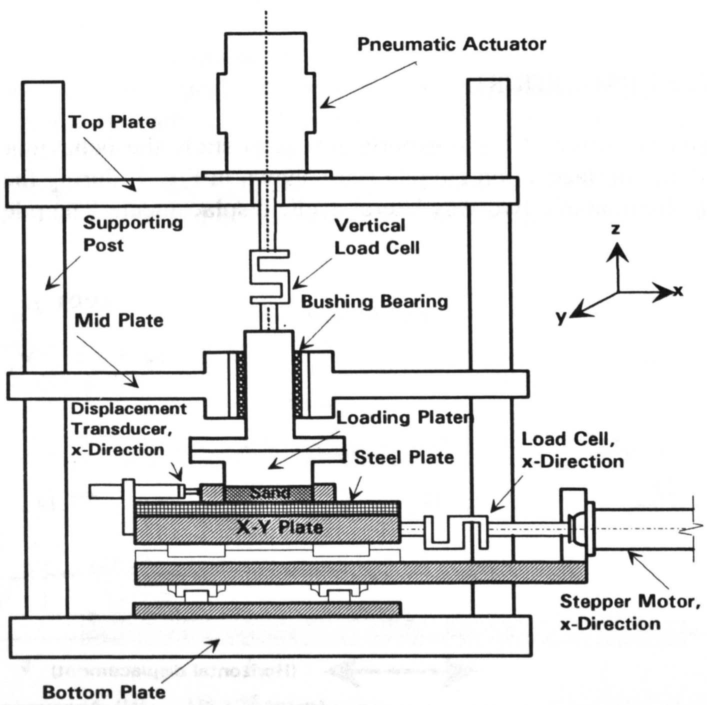

FIG. 1. Schematic diagram of the 3-D interface apparatus

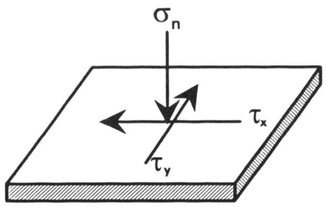

FIG. 2. Stresses applied to an interface

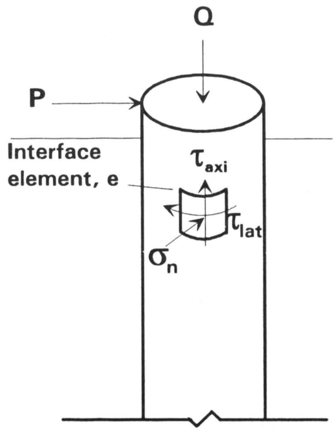

FIG. 3. An interface on an axially-laterally loaded pile

is assumed to be carrying a constant axial load which induces a shear stress, τ_y (or τ_{axi}). The lateral cyclic displacements induce a cyclic shear stress in the *x*-direction, τ_x (or τ_{lat}).

To simulate such a stress path, the interface is subjected to a constant shear stress first in the *y*-direction. The specified magnitude of τ_y is less than the peak shear stress in a monotonic test which is 80.3 *kPa* under a constant normal stress of 100 *kPa* between a medium crushed quartz sand (D_{50} of 0.6 *mm* and D_r of 84%) and a rough surface (ALO cloth # 600) as described by Fakharian and Evgin (1995). Thereafter, the interface is subjected to a displacement controlled sinusoidal shearing with an amplitude of 0.75 *mm* and a period of 200 seconds, while the shear stress in the *y*-direction, τ_y, is maintained constant. The displacement amplitude of 0.75 *mm* corresponds to the total shear displacement, U_{xa}, and is less than the total shear displacement, 1.3 *mm*, at peak strength in monotonic loading.

3-D SIMPLE SHEAR BOX

The 2-D simple shear box which was described for its operation in the *x*-direction (Fig. 4*a*) by Fakharian and Evgin (1995) is modified by adding an actuator, a load cell, and two LVDTs, a_y and b_y, in the *y*-direction (Fig. 4*b*), perpendicular to *x*-direction. The total displacement, U_{ya}, between the top aluminum plate and the steel specimen is measured by LVDT, a_y. The shear deformation of sand, U_{yb}, is measured by LVDT, b_y, which reads the relative tangential displacement between the top and bottom aluminum pates. The slip at the sand-steel interface, U_y, is obtained from $U_y = U_{ya} - U_{yb}$.

TEST PROCEDURE

The objective of these experiments is to study the behaviour of an interface, *e*, on the pile shaft shown in Fig. 3, during the application of a two-way lateral cyclic displacement. The pile

TEST RESULTS

Four tests are conducted with τ_y maintained at 0, 20, 30, and 40 *kPa*, i.e. at 0, 1/4, 3/8, and 1/2 of the peak stress of 80.3 *kPa* in a 2-D monotonic test. For $\tau_y = 0$ case, which is a 2-D cyclic displacement controlled test, the results were illustrated by Fakharian and Evgin (1995) in Fig. 3. It was shown that the shear stress, which was 72.9 *kPa* at the end of first cycle, reached a peak of 83.0 *kPa* at cycle 12 after which the shear stress decreased and stabilized at 60 *kPa*.

The cyclic test results for the interface subjected to a constant normal stress of 100 *kPa*, and constant shear stress of 20 *kPa* in the *y*-direction, τ_y, are illustrated in Figs. 5 to 7. The shear stress-sliding displacement and shear stress-shear deformation of sand in the *x*-direction are shown in Figs. 5*a* and 5*b*, respectively. As the number of cycles increases, the mobilized shear stress increases to a peak of $\tau_{xp} = 81.7$ *kPa* at cycle 5 in the *x*-direction. Thus the total peak shear stress is :

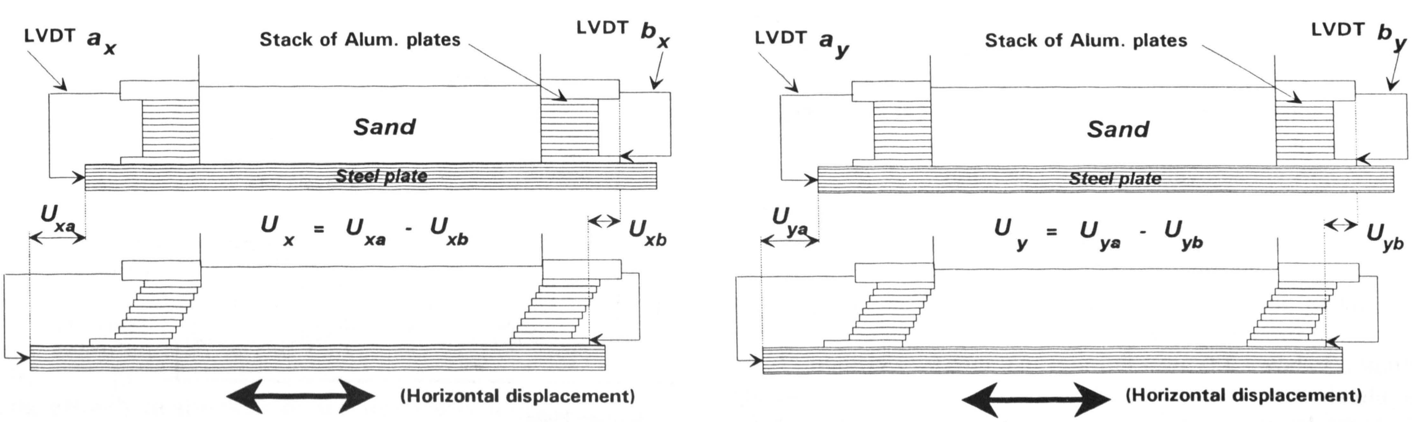

(*a*) *x-direction* (*b*) *y*-direction

FIG. 4. Schematic diagrams of shear displacements in the *x* and *y* directions

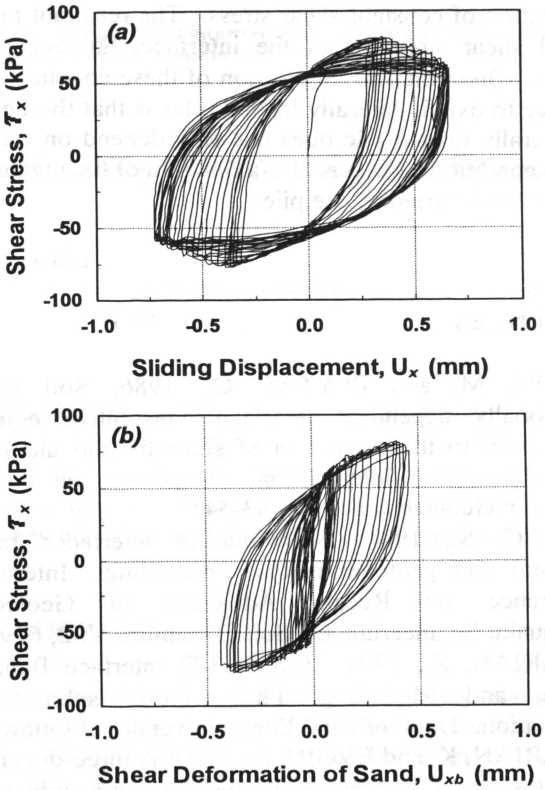

FIG. 5. Shear stress-displacement results; $\tau_y = 20\ kPa$

$$\tau_p = (\tau^2_{xp} + \tau^2_y)^{1/2} = (81.7^2 + 20.0^2) = 84.1\ kPa$$

Thereafter, the shear stress reduces and stabilizes at a residual stress of $\tau_{xres} = 59\ kPa$ in the *x*-direction. Thus the total residual shear stress is:

$$\tau_{res} = (\tau^2_{xres} + \tau^2_y)^{1/2} = (59.0^2 + 20.0^2) = 62.3\ kPa$$

Figures 5*a* and 5*b* also indicate that as the number of cycles increases, the amplitude of sliding displacement, U_x, increases and the amplitude of shear deformation of sand, U_{xb}, decreases.

The resultant shear stress versus the resultant sliding displacement is plotted in Fig. 6. It is observed that the envelope of the maximum shear stress at each cycle follows a path similar to the monotonic test results (for example, Uesugi and Kishida 1986; Fakharian and Evgin 1995).

Figure 7 shows the shear stress and sliding displacement paths on the interface plane. Figure 7*a* indicates that shear stress, τ_y, is monotonically increased to 20 *kPa* and after that it is maintained at this constant value. Subsequently, the interface is sheared in the *x*-direction in cyclic manner. The stress path in this test remains parallel to the *x*-axis at $\tau_y = 20\ kPa$. Figure 7*b* illustrates that during the displacement controlled cyclic shearing in the *x*-direction, the sliding displacement in the *y*-direction continues although shear stress, τ_y, is kept constant at 20 *kPa* in that direction. The rate of sliding displacement, U_y, increases with increasing number of cycles. Figure 7*b* also indicates that the amplitude of sliding displacement in the *x*-direction, U_x, increases when the number of cycles is increased, and eventually U_x approaches a constant value. The comparison between Figures 7*a* and 7*b* indicates that the shear stress and sliding displacement increments follow different paths on the interface plane.

Other tests with the constant τ_y at 30 and 40 *kPa* show the same trend. Table I summarizes some of the test results for different values of τ_y at 0, 20, 30, and 40 *kPa*. It is observed that at higher values of τ_y, the number of cycles required to bring the interface to a state of failure decreases. For example, at $\tau_y = 40\ kPa$, only 3 cycles are needed to fail the interface as compared to 12 cycles for $\tau_y = 0$. It is also observed that peak strength in the *x*-direction, τ_{xp}, and residual strength in that direction, τ_{xres}, decrease by increasing the magnitude of τ_y. However, the resultant peak and residual strengths (τ_p and τ_{res}) are about the same in all four cases, with an average of 82.8 *kPa* and 62.3 *kPa*, respectively.

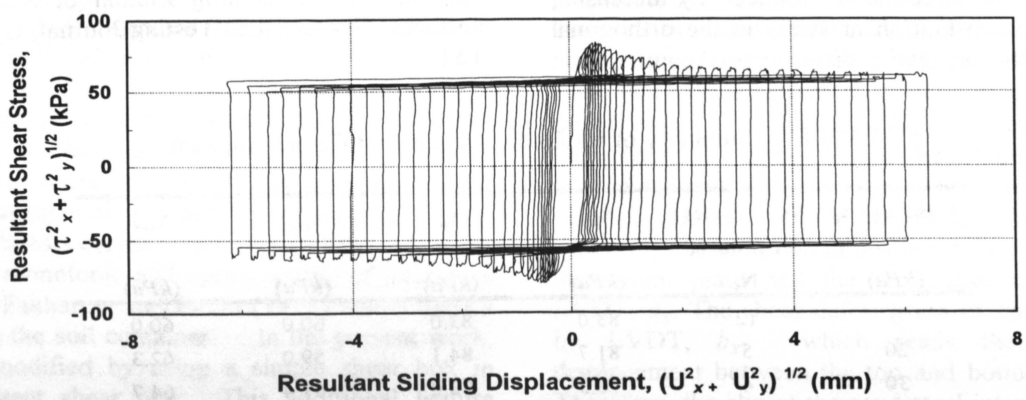

FIG. 6. Resultant shear stress-resultant sliding displacement on interface plane

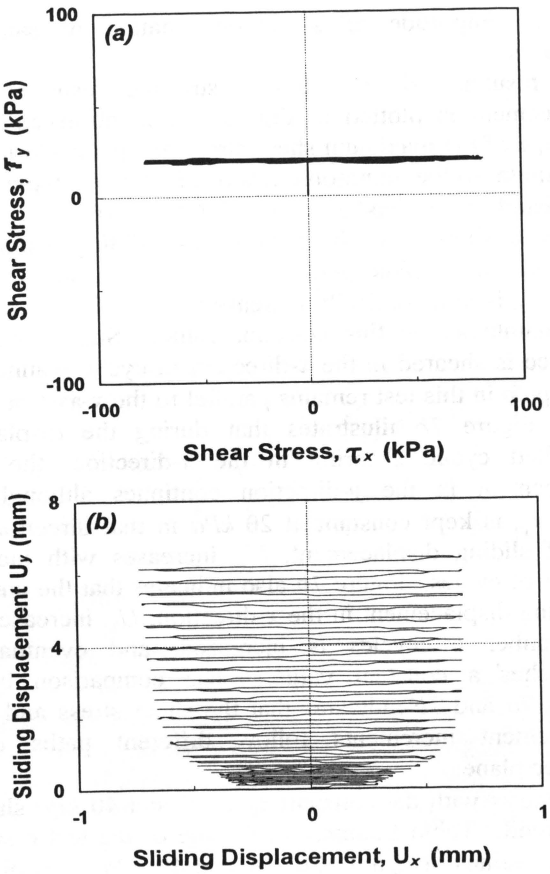

FIG. 7. Stress and displacement paths on the x-y interface plane: *(a)* shear stress paths; *(b)* sliding displacement paths

CONCLUSIONS

The experimental results presented in this study indicate that the existence of a constant shear stress significantly influences the displacement-controlled cyclic behaviour of an interface in the orthogonal direction. The number of cycles required to bring the interface to failure and the magnitude of peak and residual strengths in one direction are reduced by increasing the magnitude of the constant shear stress in the orthogonal direction. Further, the tangential displacement continues in the direction of constant shear stress. The resultant peak and residual shear strengths of the interface, however, remain constant. One practical implication of these conclusions with reference to axially-laterally loaded piles is that the behaviour of a laterally loaded pile does not only depend on the lateral loading conditions, but it is also a function of the magnitude of the axial load carried by the pile.

REFERENCES

BOULON, M. and PLYTAS, C., 1986. Soil structure directionally dependent interface constitutive equations-Application to the prediction of shaft friction along piles. Proceedings, 2nd International Symposium on numerical Models in Geomechanics, pp. 43-54.

DESAI, C. S., 1981. Behaviour of interfaces between structural and geologic media. Proceedings, International Conference on Recent Advances in Geotechnical Earthquake Engineering and Soil Dynamics, V. 2, 619-638.

FAKHARIAN, K., 1994. Cyclic 3-D Interface Behaviour: Testing and Modelling. Ph.D. thesis submitted for examination. Dept. of Civil Eng., University of Ottawa.

FAKHARIAN, K. and EVGIN, E., 1993. A three-dimensional apparatus for cyclic testing of interfaces. Proceedings, 46th Annual Canadian Geotechnical Conference, Saskatoon, Canada, pp. 485-493.

FAKHARIAN, K. and EVGIN, E., 1995. Simple shear versus direct shear tests on interfaces during cyclic loading. Proceedings, 3rd International Conference on Recent Advances in Geotechnical Earthquake Engineering and Soil Dynamics, St. Louis, Missouri, USA, April 2-7, 1995.

SMITH, T.R. and RAY, B., 1986. Shear mobilization on laterally loaded shafts. Geotechnical Aspects of Stiff and Hard Clays, Ed. Khera and Lovell, ASCE, N.Y., pp. 60-68.

UESUGI, M. and KISHIDA, H., 1986. Frictional resistance at yield between dry sand and mild steel. Soils and Foundations, 26(4), 139-149.

YOSHIMI, Y. and KISHIDA, T. ,1981. A ring torsion apparatus for evaluating friction between soil and metal surfaces. Geotechnical Testing Journal, GTJODJ, 4(4), 145-152.

TABLE I. Summary of results for tests with different constant τ_y

Constant τ_y (*kPa*)	No of cycles for failure, N_f	τ_{xp} (*kPa*)	τ_p (*kPa*)	τ_{xres} (*kPa*)	τ_{res} (*kPa*)
0	12	83.0	83.0	60.0	60.0
20	5	81.7	84.1	59.0	62.3
30	4	76.3	82.0	57.4	64.7
40	3	71.5	82.0	47.5	62.1